

Conical Fireballs, Cannon Balls And Jet-Breaks In The Afterglows Of Gamma Ray Bursts

Shlomo Dado and Arnon Dar

Physics Department, Technion, Haifa 32000, Israel

abstract. The 'jet-break' in the X-ray afterglow of gamma ray bursts (GRBs) appears to be correlated to other properties of the X-ray afterglow and the prompt gamma ray emission, but the correlations are at odds with those predicted by the conical fireball (FB) model of GRBs. They are in good agreement, however, with the correlations that are predicted by the cannonball (CB) model of GRBs.

1. Introduction

Before the launch of the Compton Gamma Ray Observatory (CGRO) in 1991 it was widely believed that gamma-ray bursts (GRBs) originate in the Galaxy or in its halo. Much larger distances together with the observed fast rise-time of GRB pulses implied an 'energy crisis' - implausible energy release in gamma rays from a very small volume in a short time, if the emission was isotropic, as was generally assumed. However, the isotropic distribution of GRBs over the sky and their intensity distribution that were measured with the Burst and Transient Source Experiment (BATSE) aboard the Compton Gamma Ray Observatory (CGRO) shortly after its launch provided a clear evidence that the observed GRBs are at very large cosmological distances (Meegan et al. 1992; Mao and Paczynski 1992). That led Shaviv and Dar (1995) to propose that GRBs are produced by inverse Compton scattering of light by highly relativistic jets whose radiation is narrowly beamed along their direction of motion and that such jets presumably are ejected following violent stellar processes such as core collapse supernovae, merger of compact stars, mass accretion on compact stars and phase transition in compact stars, rather than in spherical fireballs (Paczynski 1986, Goodman 1986) produced by neutron star merger in close binaries (Goodman et al. 1987). These jets were assumed to be a succession of highly relativistic plasmoids of ordinary matter like those observed in high resolution observations of highly relativistic jets ejected from galaxies with active galactic nucleus (e.g., M87 in Virgo), from radio galaxies (e.g., Centaurus A, the nearest radio galaxy), from quasars (e.g., 3C 273 in Virgo) and from microquasars (e.g., GRS 1915+105, SS 433, Cygnus X-1 and cygnus X-3 in our Galaxy). A key prediction of such a model was a very large linear polarization ($P \sim 100\%$) of gamma rays observed from the most probable viewing angle of the GRBs (Shaviv and Dar 1995).

The hypothesis that GRBs are produced by highly relativistic jets was not widely accepted even when the discovery of the X-ray afterglows of GRBs by the Beppo-SAX satellite (Costa et al. 1997) allowed their arcminute localization that led to the discovery of their longer wave-length afterglows (van Paradijs et al. 1997, Frail et al. 1997), host galaxies (Sahu et al. 1997) and their large redshifts (Metzger et al. 1997). In fact, the discovery of GRB afterglows, which appeared to decay like a single power-law in time, as predicted by Paczynski and Rhoads (1993), Katz (1994) and Mezaros and Rees (1997) from the isotropic fireball (FB) model (Paczynski 1986, Goodman 1986), led to an immediate wide acceptance of the relativistic isotropic fireball model as the correct description of

GRBs and their afterglows (see, e.g., Wijers et al. 1997, Piran 1999), ignoring the 'energy crisis' of the isotropic fireball model of GRBs.

When data on redshifts and afterglows of GRBs began to accumulate, it became clear that GRBs could not be explained by the isotropic fireball model (e.g., Dar 1998). Not only their large redshifts implied implausible energy release in gamma rays if the emission was isotropic, their observed afterglows seemed to behave like a smoothly broken power-law in time (Beuermann et al. 1999; Fruchter et al. 1999; Harrison et al. 1999; Kulkarni et al. 1999) rather than a single power-law. Only then, the isotropic fireball was replaced (e.g., Sari et al. 1999; Piran 2000) by an assumed conical jet of thin shells where synchrotron radiation from collisions between overtaking shells (or internal shocks) produce the observed GRB pulses, and the following collision of the merged shells with the interstellar medium (ISM) produces the synchrotron afterglow. This conical jet model which was given the name 'collimated fireball model', replaced the original fireball model, but retained its name 'the fireball model'.

The afterglow of a conical shell of opening angle θ_j , whose propagation is decelerated by sweeping up the interstellar medium (ISM) in front of it, was shown by Sari et al. 1999 to have an *achromatic break* when its bulk motion Lorentz factor $\gamma(t)$ has dropped below the value $\gamma(t) = 1/\theta_j$, which was argued to be roughly at the transition of the jet from a cone-like shape to a trumpet-like shape due to the lateral expansion of the conical jet. Moreover, the conical fireball model has been used to predict the pre-break and post-break temporal and spectral indices of the spectral energy density $F_\nu(t) \propto t^{-\alpha} \nu^{-\beta}$ of the afterglow and the *closure relations* that they satisfy.

Because of the complexity of the dynamics of spreading jets and the dependence of their afterglow on many adjustable parameters, the observed afterglows of GRBs rarely have been modeled with theoretical light-curves calculated from the conical fireball model. In most cases they were fitted with heuristic sharply or smoothly broken power-law functions connecting the pre-break and post-break behaviours predicted by Sari et al. (1999). Such heuristic functions were used primarily for convenient parametrization of the data. They allowed, however, to extract a break-time t_b from the observed light-curve and to test whether the pre-break and post break slopes satisfy the closure relations of the conical fireball model.

The jet breaks, however, were found to be chromatic (e.g., Covino et al. 2006, Panaitescu et al. 2006). The X-ray afterglows of GRBs with large equivalent isotropic energy ($E_{iso} \gg 10^{53}$ erg) that were observed with the Swift X-ray telescope (XRT) (e.g., GRBs 061007, 130427A) showed a single power-law behaviour with no visible jet break, and almost all the X-ray afterglows of less energetic GRBs that appeared to have a 'jet break' did not satisfy the closure relations of the conical fireball model, either before the break or after it (e.g., Liang et al. 2008; Racusin et al. 2009). In particular, a large fraction of the X-ray afterglows of GRBs measured with the Swift X-ray telescope (Swift/XRT) showed a canonical behaviour (Nousex et al. 2006) where the afterglow has a shallow decay phase (plateau) before the break with $\alpha(t < t_b) \ll 1$ far from the predicted $\alpha_X(t < t_b) = (3\beta_X - 1)/2$. Despite these failures and many other failures of the fireball model, the model has not been given up. Instead, the missing breaks were attributed to various reasons such as quality of

the data (Curran et al. 2008), break-time beyond the end of the Swift/XRT follow-up observations (Kocevski and Butler 2008) and far off-axis observations (Van Eerten et al. 2011a). The failure of the pre-break closure relation, to describe the shallow decay/plateau phase of canonical X-ray afterglows was attributed to an assumed continuous energy injection. The chromaticity of the jet break and the failure of the closure relation for the post-break behaviour of the X-ray afterglow were largely ignored.

In order to test whether part of the above difficulties arise from approximations used in the analytical calculations, and in order to generalize the predictions to off-axis observers, various authors have tried to derive the light-curves of conical fireballs from numerical hydrodynamical calculations. In particular, recently van Eerten and MacFadyen (2012) reported two dimensional (2D) numerical hydrodynamic calculations of the light-curves of the afterglow from conical fireballs observed from an arbitrary angle. These numerical calculations showed that the difference in the temporal indices across the jet break is larger than that predicted by Sari et al. (1999) and, contrary to expectation, it increases the discrepancy between theory and observations rather than removing it. The pre-break behaviour remains an unsolved difficulty, which was speculated to be due to an assumed continuous energy injection into the conical fireball. It was also speculated that the discrepancy between the post-break temporal slopes obtained from the numerical simulations and those observed with the Swift/XRT may be removed or reduced by assuming that the afterglow is produced by a blast wave that decelerates in a wind environment rather than in a constant density ISM.

All the above difficulties of the conical fireball (FB) model, however, were not shared by the cannonball (CB) model of GRBs: The canonical behaviour of X-ray afterglows where a plateau/shallow decay phase is smoothly broken to a steep power-law decline was predicted long before it was observed with Swift/XRT (see, e.g., Figs. 6, 26-30 in Dado et al. 2002; see also Dado et al. 2009a,b for a detailed comparison between the light-curves of the X-ray afterglows of GRBs measured with Swift/XRT and those predicted by the CB model). The post-break closure relations predicted by the CB model were also shown to be well satisfied by the Swift/XRT light curves (Dado and Dar 2012a).

The failures of the standard conical fireball model, however, did not appear to shake the wide belief in this model or in its interpretation of the afterglow breaks. Hence, in this paper we present additional *parameter-free* tests of the origin of the observed break in the light-curve of canonical X-ray afterglows of GRBs. Namely, we compare the observed correlations between the jet breaks in the X-ray afterglows of GRBs measured with the Swift/XRT between December 2004 and December 2012 and the prompt gamma-ray emission properties of these GRBs, and those predicted by the conical fireball and cannonball models. We limit our tests to the X-ray afterglow, in order to avoid dependence on adjustable parameters. This extends our preliminary study of missing breaks in the X-ray afterglows of GRBs (Dado et al 2007) that was based on limited statistics. For completeness, the derivation of the break properties from the conical fireball model and from the cannonball model are presented in Appendixes A1 and A2, respectively.

2. Jet Break Correlations

2.1. Conical jet break

In standard conical jet models of GRBs, $1/\gamma(0) \ll \theta_j$. The break in the afterglow occurs when the beaming angle $1/\gamma(t)$ of the emitted radiation from the decelerating jet in the interstellar medium (ISM) becomes larger than the opening angle θ_j of the conical jet, i.e., when $1/\gamma(t_b) \approx \theta_j$. For a conical jet at redshift z with kinetic energy E_k propagating in an ISM with a constant baryon density n_b , the break is observed by a distant observer on/near axis at a time (see Appendix A)

$$t_b \approx \frac{(1+z)}{8c} \left[\frac{3E_k}{2\pi n_b m_p c^2} \right]^{1/3} \theta_j^2. \quad (1)$$

Eq. (1) is the relation derived by Sari et al. (1999) for a conical shell which begins rapid lateral spreading on top of its radial motion when $\gamma(t) \approx 1/\theta_j$.

If the jets that produce GRBs had approximately a standard ISM environment and a standard E_k (Frail et al. 2001), then Eq.(1) would have yielded the correlation

$$t'_b \propto [E_{iso}]^{-1}, \quad (2)$$

where E_{iso} is the total gamma-ray energy emission under the assumption of isotropic emission.

Because $1/\gamma(0) \ll \theta_j$, the highly relativistic conical ejecta and its beamed gamma-ray emission share the same cone. Since the observed spectrum of GRBs is given roughly by a cutoff power-law (CPL) $E dn_\gamma/dE \propto e^{-E/E_p}$, the assumption of the conical fireball model that a constant fraction of the jet kinetic energy is converted to gamma-ray energy implies that

$$E'_p \propto \frac{E_k}{\pi \theta_j^2} \propto E_{iso}, \quad (3)$$

where E'_p is the peak energy of the time-integrated observed spectral energy flux. Consequently, the fireball model assumptions yield also the binary correlation $t'_b \propto [E'_p]^{-1}$.

Note also that for a ballistic (non spreading) conical jet viewed on/near-axis, the power-law decline of the X-ray afterglow of an isotropic fireball seen by a distant observer is multiplied by a factor

$$K_b = \left[1 - \frac{1}{(1 + \gamma^2 \theta_j^2)^{\beta_X + 1}} \right], \quad (4)$$

which follows from Eq. (A.6) of Appendix A1 for $\theta_j^2 \ll 1$. For $t \ll t_b$, $\gamma^2 \theta_j^2 \gg 1$ and $K_b \approx 1$, while for $t \gg t_b$, $\gamma^2 \theta_j^2 \ll 1$ and $K_b \approx (\beta_X + 1) \gamma^2 \theta_j^2 \propto t^{-3/4}$. Hence, the temporal index α of the afterglow of a conical jet increases by $\Delta\alpha = 0.75$ across the break, independent of the spectral index β_X and the pre-break temporal index of the afterglow.

In the case of a wind-structured environment with a density profile $n(r) = n_0 R_0^2/R^2$, the power-law indices of the $t'_b - E_{iso}$ and $t'_b - E'_p$ correlations are identical to those for an ISM circumburst environment (see Appendix A1).

Moreover, although the $t'_b - E_{iso}$ and $t'_b - E'_p$ correlations were derived for the case where no continuous energy injection during the plateau phase of the X-ray afterglow takes place,

they are valid also, to a good approximation, when continuous energy injection is invoked. This is because the injected energy during the afterglow phase must be much smaller than the initial kinetic energy which powers the prompt gamma-ray emission whose energy is much larger than that of the afterglow. Since the afterglow is only partially powered by the assumed continuous energy injection, the continuous energy injection must be rather small compared to E_k , the total kinetic energy of the jet. Hence, the assumption, $E_{iso} \propto E_k$ holds to a good approximation and Eq. (A.1) implies that the correlations derived from Eq. (A.1) are valid also when such a continuous energy injection after the prompt emission phase is present.

2.2. Cannonball deceleration break

In the CB model of GRBs a succession of initially expanding plasmoids (CBs) of ordinary matter merge into a slowly expanding ($(kT/m_p \gamma^2)^{1/2} \ll c$) leading CB with a large bulk motion Lorentz factor, $\gamma(0) \sim 10^3$, that decelerates in collision with the circumburst medium/ISM. The emitted synchrotron radiation is relativistically beamed along its direction of motion, redshifted by the cosmic expansion and its arrival time in the frame of a distant observer at a viewing angle θ relative to the direction of motion of the CB is aberrated (e.g., Dar and De Rújula 2004 and references therein). The rate of change in the bulk motion Lorentz and Doppler factors of the CB due to the deceleration of the CB in the circumburst medium is small until the swept-in mass by the CB becomes comparable to its initial mass. This happens in the observer frame at a time (see, e.g., Dado et al. 2009a and references therein)

$$t_b \approx \frac{(1+z) N_b}{8 c n_b \pi R^2} \frac{1}{\gamma_0 \delta_0^2}, \quad (5)$$

where N_b is the baryon number of the CB and R is its radius. The rapid decrease of $\gamma(t)$ and $\delta(t)$ beyond t_b produces a smooth transition (break) around t_b of the observed spectral energy density $F_\nu(t) \propto [\gamma(t)]^{3\beta-1} [\delta(t)]^{\beta+3} \nu^{-\beta}$ of the emitted afterglow from a plateau phase to an asymptotic power-law decline (e.g., Dado et al. 2002, 2009a and references therein).

In the CB model, $E'_p \propto \gamma_0 \delta_0$ and $E_{iso} \propto \gamma_0 \delta_0^3$, respectively. Consequently, Eq. (5) yields the triple correlation,

$$t'_b \propto [E'_p E_{iso}]^{-1/2}. \quad (6)$$

Moreover, substituting the CB model approximate binary power-law correlation $E'_p \propto [E_{iso}]^{1/2}$ into the triple $t'_b - E'_p - E_{iso}$ correlation yields the $t'_b - E_{iso}$ and $t'_b - E'_p$ binary correlations,

$$t'_b \propto [E_{iso}]^{-3/4} \propto [E'_p]^{-3/2}, \quad (7)$$

where a prime indicates the value in the GRB rest frame. Naturally, these approximate correlations are expected to have a larger spread than the original triple $t'_b - E'_p - E_{iso}$ correlation.

In the case of a wind-like density, which extends typically beyond the end of the glory region at $R_g \sim 10^{16}$ cm (Dado et al. 2009) and up to $R_w \sim 5 \times 10^{17}$ cm where the wind

density decreases below $\sim m_p/rmcm^3$ (for the wind parameters listed in Appendix A1), the predicted spectral energy flux of the afterglow has the behaviour $F_\nu(t) \propto t^{-(\beta+1)} \nu^{-\beta}$ where $\beta(t)$ is the spectral index in the observed band (see, e.g., Dado et al. 2009). The observed crossing time of such a wind region is roughly $(1+z)R_w/\gamma_0\delta_0$, typically $< 50(1+z)$ s because γ and δ change little during the wind crossing. Beyond the wind region, $F_\nu(t)$ in the X-ray band has the standard canonical behaviour of X-ray afterglows in the CB model in an ISM environment, i.e., with an afterglow break/bend at the end of a plateau phase that satisfies Eq. (7).

3. Comparison with observations

Fig. 1 presents the best fit power-law to the observed $E'_p - E_{iso}$ correlation using an unbiased sample of 110 GRBs with known redshift measured before January 1, 2013. The values of E'_p and E_{iso} were compiled from communications of the Konus-Wind and Fermi GBM collaborations to the GCN Circulars Archive (Barthelmy 1997), and from publications by Amati et al. (2007,2008), Yonetoku et al. (2010), Gruber et al. (2011), Nava et al. (2012) and D'Avanzo et al. (2012). Using essentially the method advocated by D'Agostini (2005), we obtained the best fit power-law correlations $E'_p \propto [E_{iso}]^{0.54}$ in good agreement with $E'_p \propto [E_{iso}]^{1/2}$ predicted by the CB model but in disagreement with $E'_p \propto E_{iso}$ expected in the conical fireball model.

Fig. 2 compares the triple correlation $t'_b - E'_p - E_{iso}$ predicted by the CB model (Eq. 6) and the observed correlation in 70 Swift GRBs (Evans et al. 2009) from the above GRB sample, which have a good Swift/XRT temporal sampling of their X-ray afterglow during the first day (or more) following the prompt emission phase and have no superimposed flares. In this sample the X-ray afterglow of 55 GRBs clearly show a break and no afterglow-break was observed in 15 GRBs. The upper bound on a possible early time break for the 15 GRBs with no visible break are indicated by down pointing arrows. Also shown is the late-time break of the X-ray afterglow of GRB 980425, which was measured with Chandra (Kouveliotou et al. 2004). In order not to bias the values of t_b by the CB model fits, the break times were taken to be the times of the first break with $\alpha(t < t_b) < \alpha(t > t_b)$ obtained from a broken power-law fit to the GRB X-ray afterglow measured with the Swift/XRT and reported in the Leicester XRT GRB catalog (Evans et al. 2009) or from their smoothly broken power-law fits of Margutti et al. (2013). The Spearman rank (correlation coefficient) of the triple correlation $t'_b - (E'_p E_{iso})$ for the subsample of 55 GRBs with a visible break is $r = -0.74$ corresponding to a chance probability less than 1.4×10^{-10} . The best fit triple correlation $t'_b \propto [E'_p E_{iso}]^q$ that was obtained for the subsample of 55 GRBs using essentially the maximum likelihood method advocated by D'Agostini (2005), yields $q = -0.58 \pm 0.04$.

The approximate binary correlations $t'_b - E_{iso}$ and $t'_b - E'_p$ that were obtained by substitution of the CB model predicted correlation $E'_p \propto [E_{iso}]^{1/2}$ in the triple correlation $t'_b - E'_p - E_{iso}$ (Eq. 6) are compared with the observational data in Figs. 3 and 4, respectively. GRB 980425 was excluded from the GRB sample because in the CB model the $E'_p \propto [E_{iso}]^{1/2}$ is satisfied only by ordinary GRBs where $\theta \approx 1/\gamma$, while far-off axis GRBs such as 980425 with $\theta \gg 1/\gamma$ satisfy $E'_p \propto [E_{iso}]^{1/3}$, i.e., they are outliers with respect to

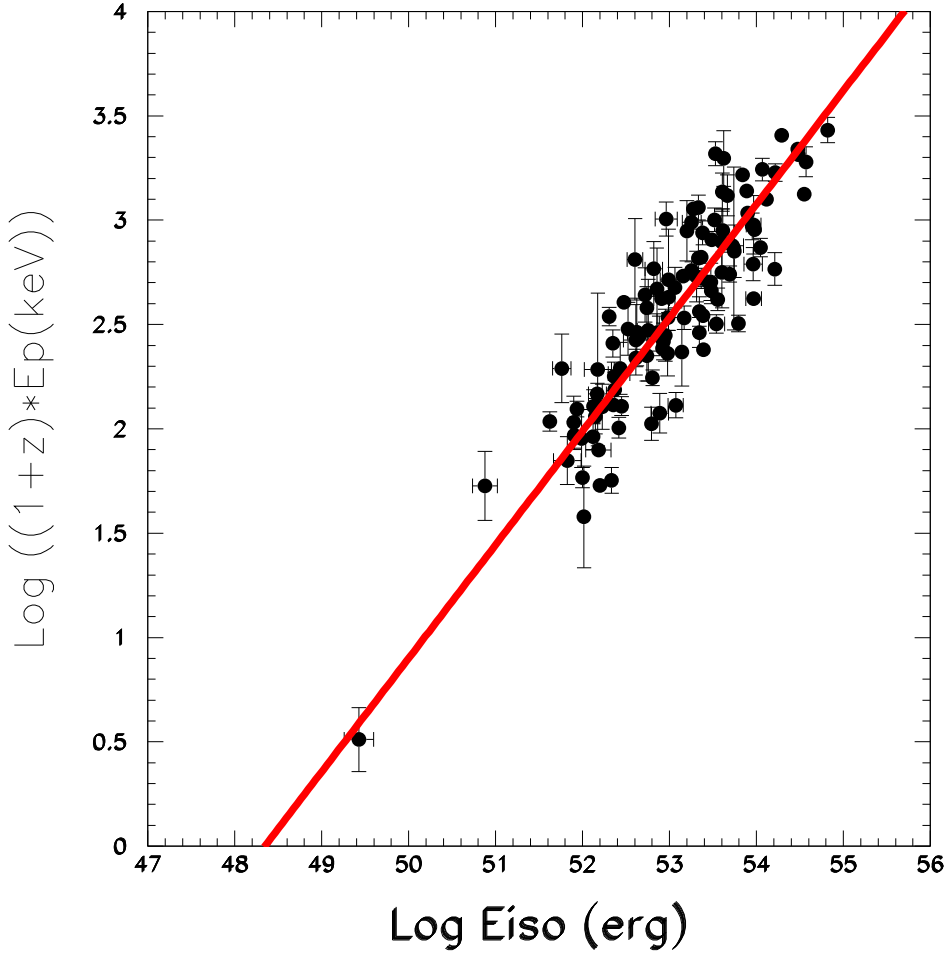


Fig. 1. The observed correlation between E'_p and E_{iso} for 121 long GRBs with known redshift. The best fit power-law correlation (straight line) has a power-law index 0.54.

the assumed $E'_p \propto [E_{iso}]^{1/2}$ correlation. The Spearman ranks of the observed $t'_b - E_{iso}$ and $t'_b - E'_p$ correlations are -0.49 and -0.63 with chance probabilities less than 4.5×10^{-4} and 1.0×10^{-6} , respectively, and as expected (in the CB model), they are larger than that of the $t'_b - (E'_p E_{iso})$ correlations. The best fit power-law indices of the $t'_b - E_{iso}$ and $t'_b - E'_p$ correlations are -0.70 ± 0.06 and -1.64 ± 0.04 , respectively, consistent with their predicted values by the CB model, -0.75 and -1.50 , respectively.

A comparison between the best fit indices of the break-time power-law correlations and those expected in the CB and FB models is summarized in Table 1 for the sample of 55 Swift GRBs with a visible afterglow break. As can be seen from Table 1, the values of the power-law correlation indices predicted by the CB model are consistent with those obtained from the best fits. The best fit indices, 0.54 ± 0.01 , -0.69 ± 0.06 and -1.62 ± 0.04 of the observed $E'_p - E_{iso}$, $t'_b - E'_p$ and $t'_b - E_{iso}$ power-law correlations, however, are at odds with the values 1, -1, and -1, respectively, expected in the conical fireball model. While the χ^2/dof of the predicted correlations by the CB model differ from those of the best fits by

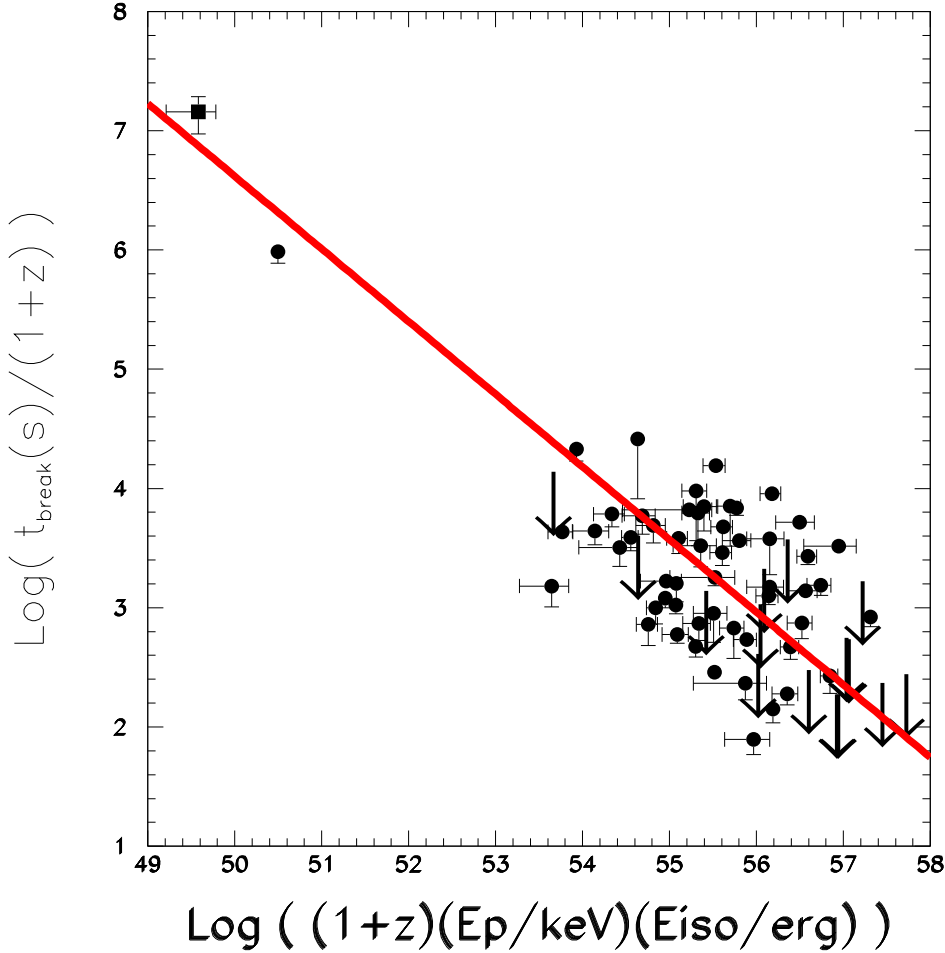


Fig. 2. The observed triple correlations $t'_b - E'_p - E_{iso}$ in 70 Swift GRBs with measured redshift, t'_b , E'_p , and E_{iso} and its best fit power-law (straight line with a power-law index - 0.58). Arrows indicate observational upper bounds on early-time deceleration breaks before the beginning of the Swift/XRT observations or hidden under the prompt emission tail. The square represents the break in the late-time X-ray afterglow of GRB 980425 which was observed with Chandra.

less than $1/dof$, the χ^2/dof of the predicted correlations by the FB model differ by much larger values, as summarized in Table 2.

The correlations satisfied by t'_b imply that GRBs with very large E_{iso} and/or E'_p have a break at small t'_b , which is hidden under the tail of the prompt emission or precedes the start of the Swift/XRT follow up observations (Dado et al. 2007). Indeed, the X-ray afterglow of all the 15 GRBs in the sample, which have a very large $E_{iso} \times E'_p$, have a single power-law decline consistent with the post-break power-law decline predicted by the CB model (see, e.g., Dado et al. 2007, 2009a). For such GRBs, the observations provide only upper bounds for the break-times of their X-ray afterglows. The correlations satisfied by t'_b imply that GRBs with very large $E_{iso} \times E'_p$ have a break at small t'_b , which is hidden under the tail of the prompt emission or precedes the start of the Swift/XRT follow up

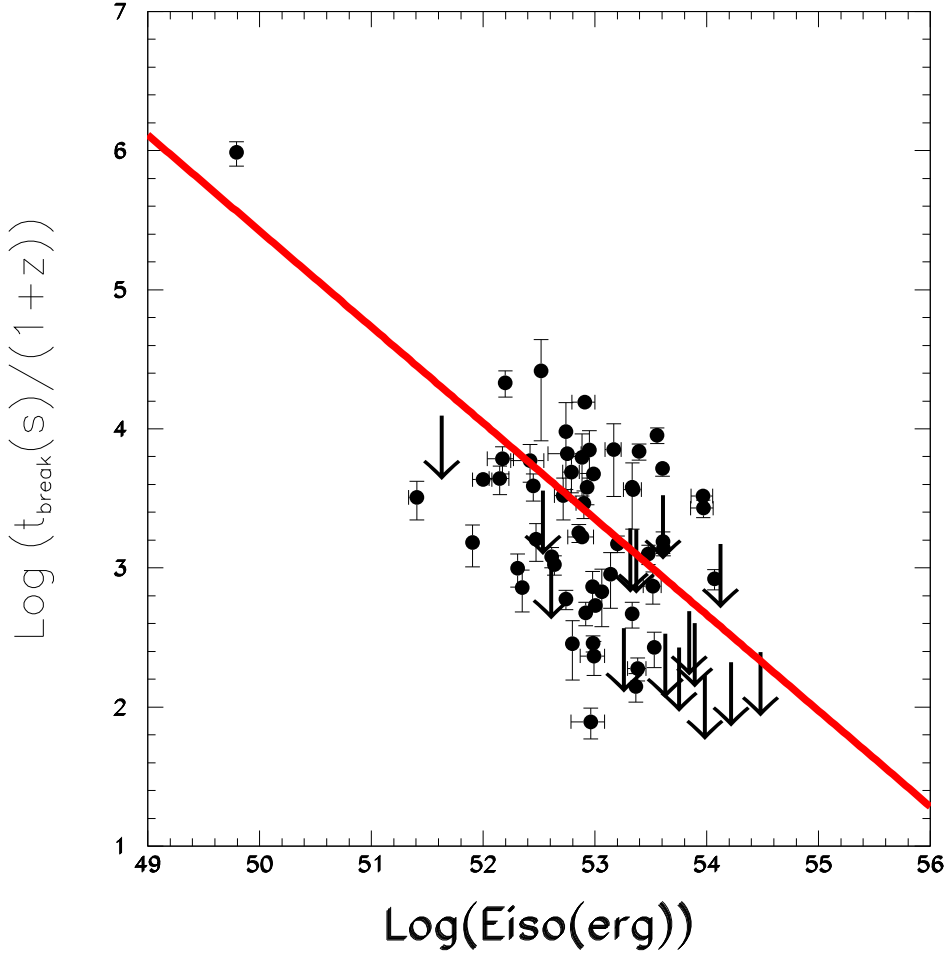


Fig. 3. Comparison between the binary correlation $t'_b - E_{iso}$ predicted by the CB model (Eq. 7) and that observed in 70 Swift GRBs with known redshift, t'_b and E_{iso} . Arrows indicate observational upper bounds on early time deceleration breaks before the beginning of the Swift/XRT observations or hidden under the prompt emission tail.

observations (Dado et al. 2007). Indeed, the X-ray afterglow of all the 15 GRBs in the GRB sample, which have a very large E_{iso} , and/or E'_p , have a single power-law decline consistent with the post-break power-law decline predicted by the CB model (see, e.g., Dado et al. 2007, 2009a). For such GRBs, the observations provide only upper bounds for the break-times of their X-ray afterglows.

However, for most of the 15 GRBs with only an upper bound on their afterglow break-time, which are indicated by down pointing errors in Figs. 2-4, an early break-time value was extracted from a CB model fit to the entire X-ray light curve, which includes the fast decline phase of the prompt emission and the afterglow component (see, e.g., Dado et al. 2009). Replacement of the upper bounds by the CB model fitted break-times (which could have biased the break-times values) and their inclusion in the best fits had very little effect on the values of the best fit power-law indices and their errors.

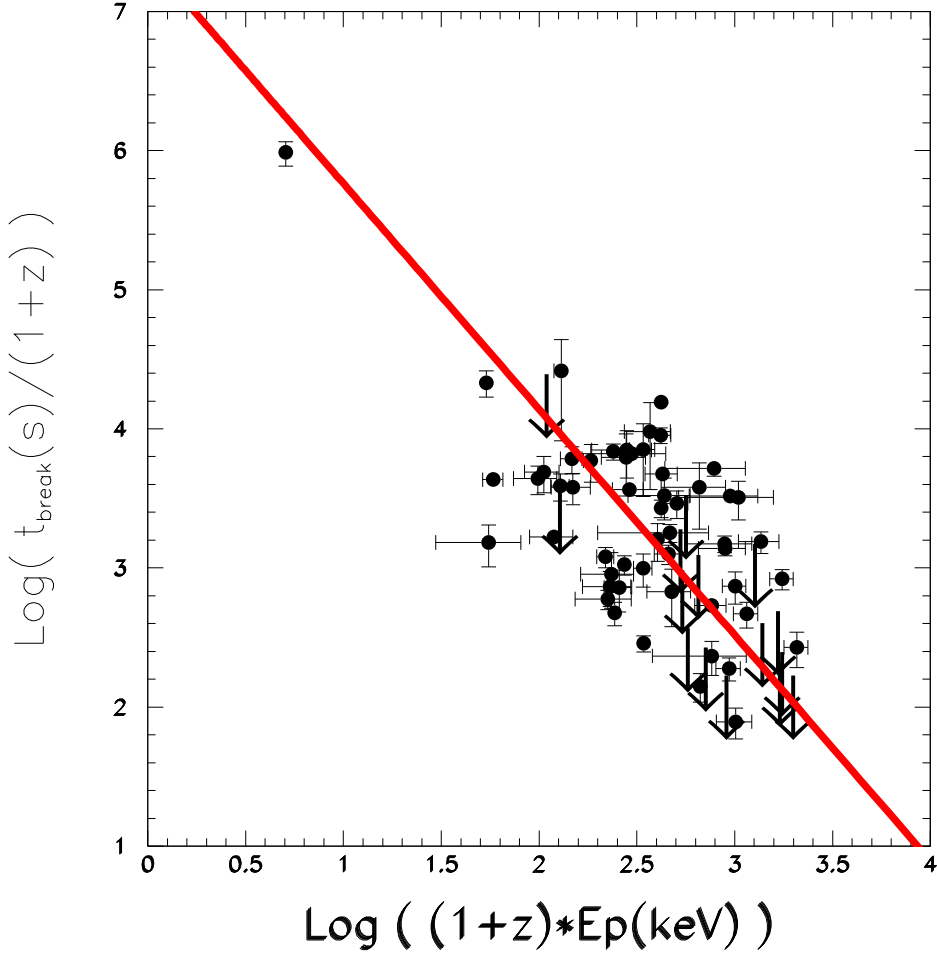


Fig. 4. Comparison between the binary correlation $t'_b - E'_p$ predicted by the CB model (Eq. 7) and that observed in 70 Swift GRBs with known redshift, t'_b and E'_p . Arrows indicate observational upper bounds on early time deceleration breaks which may have taken place before the beginning of the Swift/XRT observations or are hidden under the prompt emission tail.

4. Conclusions and discussion

Correlations and closure relations between GRB properties that are predicted by GRB models allow parameter-free tests of such models. In particular, comparison between the observed and predicted correlations between the 'jet break' in the X-ray afterglow of GRBs and the prompt gamma-ray emission, like the $E'_p - E_{iso}$ correlation, allow another critical test of the conical fireball model and the cannonball model of GRBs. Although the 'jet break' in the afterglow of GRBs has been the flagship of the conical fireball model, the observed correlations between the 'jet break' in the X-ray afterglow of GRBs measured with the Swift/XRT and their prompt gamma-ray emission are inconsistent with those expected in the conical fireball model. This failure, perhaps is not a surprise since the observed 'jet-breaks' were found before to be chromatic, the predicted pre-break and post-break temporal behaviours and closure relations were found to be badly violated, and the

Table 1. Summary of the observed power-law correlations between E'_p , E_{iso} and t'_b and their power-law indices expected in the Cannonball (CB) and collimated fireball (FB) models. ρ is the Spearman rank (correlation coefficient), $P(\rho)$ is the chance probability of a correlation coefficient $\geq \rho$, and p is the power-law index of the power-law correlation.

Correlation	ρ	$P(\rho)$	$p(\text{fit})$	$p(\text{CB})$	$p(\text{FB})$
$E'_p - E_{iso}$	+0.87	~ 0	$0.54 \pm .01$	1/2	1
$t'_b - (E'_p E_{iso})$	-0.74	1.3×10^{-10}	$-0.58 \pm .04$	-1/2	
$t'_b - E'_p$	-0.63	1.0×10^{-6}	$-1.62 \pm .04$	-3/2	-1
$t'_b - E_{iso}$	-0.49	4.5×10^{-4}	$-0.69 \pm .06$	-3/4	-1

Table 2. The χ^2/dof statistic for the best fit power-law correlations between E'_p , E_{iso} and t'_b and for the correlations predicted by the cannonball (CB) and collimated fireball (FB) models.

Correlation	dof	best fit	CB	FB
$E'_p - E_{iso}$	108	19.2	20.2	99.7
$t'_b - (E'_p E_{iso})$	53	26.9	27.5	—
$t'_b - E'_p$	53	22.3	23.1	27.6
$t'_b - E_{iso}$	53	23.0	24.6	30.1

observed change in slope across the breaks is not that predicted. The replacement of the approximate analytical estimates in the conical fireball model (Sari et al. 1999) by more exact hydrodynamical calculations (e.g. van Eerten and MacFadyen 2012) does not change the situation. They neither reproduce the observed correlations, nor do they remove the discrepancies between the predicted and observed pre-break and post break behaviours of the afterglows. These failures provide additional evidence that GRBs and their afterglows are not produced by conical jets, the so called 'collimated fireballs'.

In contrast, the correlations between the deceleration break in the afterglow of GRBs and their prompt γ -ray emission predicted by the cannonball model are in good agreement with those observed, as shown in Figs 1-4. The correlations between the break and other afterglow properties predicted by the cannonball model (Dado and Dar 2012b), as well as the pre-break and post-break behaviours of the light curves of the X-ray afterglow, were shown to accord well with the observations (e.g., Dado et al. 2009, Dado and Dar 2012a). Moreover, in the CB model, the $t'_b - (1+z)$ 'anti-correlation' noted by Stratta et al. (2009), is a simple consequence of beaming and the detection threshold, which enrich the low z GRB sample with far-off-axis soft GRBs and X-Ray Flashes (e.g., Dado et al. 2004) relative to the high z events that must be much harder and energetic in order to be detected. These selection effects that produce the effective $\langle E'_p(z) \rangle - z$ and $\langle E_{iso}(z) \rangle - z$ 'correlations' result in an effective $t'_b(z) - z$ 'anti-correlation' (Dado and Dar, in preparation).

Appendix A: Ballistic conical shells

Consider the deceleration of a highly relativistic conical shell of a solid angle $2\pi(1 - \cos\theta_j) \approx \pi\theta_j^2$ that expands radially and decelerates by sweeping in the medium in front of it.

Assuming a plastic collision and neglecting radiation losses, relativistic energy-momentum conservation, $d(M\gamma) = 0$, can be written as,

$$\frac{M_0 \gamma_0}{\gamma} d\gamma = -\gamma^2 \pi \theta_j^2 n_b m_p R^2 dR, \quad (\text{A.1})$$

where $M(t) = M_0 \gamma(0)/\gamma$ is the mass of the jet, $M_0 = M(0)$, $\gamma_0 = \gamma(0)$, n_b is the constant baryon density of the external medium, and $R(t)$ is the radius of the conical shell. Eq. (A.1) yields

$$[R^3 - R_0^3] = \frac{3 M_0 \gamma_0}{2 \pi \theta_j^2 n m_p} \left[\frac{1}{\gamma^2} - \frac{1}{\gamma_0^2} \right]. \quad (\text{A.2})$$

In the conical fireball model, ordinary GRBs have $\gamma_0^2 \theta_j^2 \gg 1$, whereas $\gamma(t'_b) \theta_j \approx 1$ at the break-time t'_b in the GRB rest frame corresponding to a break-time t_b in the observer frame. Consequently, Eq. (A.1) implies that the radius of the conical shell at t'_b is given by

$$R_b = R(t'_b) \approx \left[\frac{3 E_k}{2 \pi n m_p c^2} \right]^{1/3}, \quad (\text{A.3})$$

where $E_k \simeq M_0 \gamma_0 c^2$ is the kinetic energy of the conical ejecta. Eq. (A.1) yields also the asymptotic behaviour $R \approx c t' \approx R_b [\gamma(t')/\gamma_b]^{-2/3}$, which is reached already well before t'_b . Because of time aberration and cosmic expansion, the on-axis observer's time interval dt that corresponds to the time interval $dt' = dR/c$ in the GRB rest frame is given by $dt = (1+z) dt'/2\gamma^2$. Consequently, $\gamma(t')$ has the asymptotic behaviour $\gamma_b (t/t_b)^{-3/8}$ where the observed on-axis break-time is given by

$$t_b = \int^{t'_b} dt = (1+z) \int^{t'_b} \frac{dt'}{2\gamma^2} \approx \frac{(1+z) R_b \theta_j^2}{8c}, \quad (\text{A.4})$$

and where we have assumed that most of the contribution to the integral comes from times when $\gamma(t') = \gamma_b (t'/t'_b)^{-3/2}$ is already a good approximation.

If the total gamma-ray energy emitted in GRBs is a constant fraction of the initial kinetic energy of the conical shell, $E_\gamma = \eta E_k$, which in the conical fireball model is related to the isotropic equivalent gamma-ray energy E_{iso} of the GRB by ¹ $E_{iso} \approx 4 E_\gamma / \theta_j^2$ then

$$t_b = \frac{(1+z)}{16c} \left[\frac{3 E_{iso}}{\pi \eta n m_p c^2} \right]^{1/3} \theta_j^{8/3}. \quad (\text{A.5})$$

Eqs. (A.4, A.5) were used by Sari et al. (1999) to represent conical jets with lateral expansion.

A distant observer sees only the beamed radiation from an area $R^2 \pi / \gamma^2$ along the line of sight of a spherical shell or a conical shell. Consequently, as long as $\gamma(t) > 1/\theta_j$ the observed afterglows from a conical fireball or an isotropic fireball have the same visible area. Beyond the break the visible area of a spherical fireball continues to be $\approx R^2 \pi / \gamma^2$, while that of a conical shell becomes $\approx R^2 \pi \theta_j^2$. Hence the light-curve of the afterglow of the conical fireball beyond the break is steeper by their ratio $\gamma^2 \theta_j^2 \approx (t/t_b)^{-0.75}$, where we used the asymptotic behaviour $\gamma(t) = \gamma_b (t/t_b)^{-3/8}$ in a constant density environment and $\gamma_b = 1/\theta_j$. This steepening of the power-law decline by $\Delta\alpha = 0.75$ across the break independent of β is

¹ The solid angle of a conical shell is $\Omega_j = 2\pi(1 - \cos\theta_j)$, which yields a beaming factor $f_b = 2\pi(1 - \cos\theta_j)/4\pi = (1 - \cos\theta_j)/2$, and not $f_b = (1 - \cos\theta_j)$ that is widely used in the GRB literature.

different from that derived by Sari et al. (1999) for a spreading jet. The smooth transition between the pre-break and post-break power laws can also be derived more rigorously: Relativistic beaming and Doppler boosting modulates the observed emission from every point on the conical shell by a factor $\delta^{1+\Gamma}$ where $\delta = 1/\gamma(1 - \beta \cos\theta)$ is the Doppler factor on the shell at an angle θ relative to the line of sight to the observer, $\beta = v/c$ and Γ is the photon spectral index of the radiation. For isotropic medium, isotropic conical shell and isotropic expansion, this is the only dependence of the received radiation on the line of sight to the observer. Consequently, the observed energy-flux (at a given energy) of photons emitted simultaneously by the conical shell is modulated by the factor

$$I(\gamma, \theta_j) = 2\pi \int \delta^{\Gamma+1} d\cos\theta = \frac{2\pi}{\beta\gamma\Gamma} \left[\frac{1}{(1-\beta)^\Gamma} - \frac{1}{(1-\beta\cos\theta_j)^\Gamma} \right]. \quad (\text{A.6})$$

The difference in arrival times of photons emitted simultaneously from the conical shell was ignored in the above analytical estimates of the break-time and the spectral index change across the break. The spread in arrival times has no effect on E_{iso} , it is $\Delta t \approx R/2c\gamma^2$ before the break and $\Delta t \approx R\theta_j^2/c$ after the break. Thus, Δt is roughly 4 times larger than t before the break but smaller than t by a factor $4\gamma^2\theta_j^2 \ll 1$ at late times. The spread in arrival time that has a negligible effect on E_{iso} and $\Delta\alpha$ cannot be neglected in estimating t_b . The same conclusion is valid also for the effects of off-axis viewing when the viewing angle θ is not negligible compared to θ_j . Generally, the effects of off-axis viewing and the spread in arrival time require numerical integrations (e.g., van Eerten and MacFadyen 2012) and make the widely used simple relation, Eq. (A.4) a very rough estimate.

If the typical circumburst region of LGRBs is the wind region of a Wolf Rayet star that blows a constant wind, than its density profile is $\rho = \rho_0 R_0^2/R^2 = \dot{M}/4\pi R^2 V$ where the typical mass-loss rate $\dot{M} \sim 10^{-4} M_\odot \text{y}^{-1}$ and the typical wind velocity $V \sim 1000 \text{ km s}^{-1}$ yield $\rho_0 R_0^2 = 5 \times 10^{11} \text{ g cm}^{-1}$. The replacement of $n_b m_p R^2$ with $\rho_0 R_0^2$ in the Eq. (A.1), and repetition of the derivations of the break-time correlations for a constant density, yield for $\gamma\theta = 1$

$$R_b \approx \frac{E_k}{2\pi \rho_0 R_0^2 c^3} \quad (\text{A.7})$$

i.e., a typical $R_b \approx 3.5 \times 10^{16}$ independent of θ , and

$$t'_b \approx \frac{\theta^2 E_k}{8\pi \rho_0 R_0^2 c^3} = \frac{\eta E_k^2}{2\pi \rho_0 R_0^2 c^3} \frac{1}{E_{iso}}. \quad (\text{A.8})$$

Hence, the break-time power-law correlations for ISM and wind-like density profiles have identical power-law indices, i.e., $t'_b \propto 1/E_{iso} \propto 1/E'_p$.

Appendix B: Ballistic cannonballs

In the cannonball model the electrons that enter the CB are Fermi accelerated and cool rapidly by synchrotron radiation (SR). This SR is isotropic in the CB's rest frame and has a smoothly broken power-law spectrum with a characteristic bend/break frequency, which is the typical synchrotron frequency radiated by the interstellar medium (ISM) electrons that enter the CB at time t with a relative Lorentz factor $\gamma(t)$. In the observer frame, the emitted photons are beamed into a narrow cone along the CB's direction of motion

by its highly relativistic bulk motion, their arrival times are aberrated and their energies are boosted by its bulk motion Doppler factor δ and redshifted by the cosmic expansion during their travel time to the observer. For the X-ray band that is well above the break frequency, the CB model yields the spectral energy density (see, e.g., Eq. (26) in Dado et al. 2009a),

$$F_\nu \propto n^{(\beta_X+1)/2} [\gamma(t)]^{3\beta_X-1} [\delta(t)]^{\beta_X+3} \nu^{-\beta_X}. \quad (\text{B.1})$$

For a CB of a baryon number N_B , a constant or slowly expanding radius R and an initial Lorentz factor $\gamma_0 = \gamma(0) \gg 1$, which propagates in an ISM of a constant density n_b , relativistic energy-momentum conservation yields the deceleration law (Dado et al. 2009b and references therein)

$$\gamma(t) = \frac{\gamma_0}{[\sqrt{(1+\theta^2\gamma_0^2)^2 + t/t_0} - \theta^2\gamma_0^2]^{1/2}}, \quad (\text{B.2})$$

where $t_0 = (1+z)N_B/8cn\pi R^2\gamma_0^3$. As long as $t < t_b = (1+\gamma_0^2\theta^2)^2 t_0$, $\gamma(t)$ and $\delta(t)$ change rather slowly with t , which generates the plateau phase of $F_\nu(t)$ of canonical X-ray AGs that was predicted by the CB model (see, e.g., Dado et al. 2002, Figs. 6, 27-33) and later observed with Swift (Nousek et al. 2006). For $t \gg t_b$, $\gamma(t) \rightarrow \gamma_0(t/t_b)^{-1/4}$, $[\gamma(t)\theta]^2$ becomes $\ll 1$ and $\delta \approx 2\gamma(t)$, which result in a post-break power-law decline

$$F_\nu(t) \propto \nu^{-\beta_X} t^{-(\beta_X+1/2)}. \quad (\text{B.3})$$

Thus, in the CB model, the asymptotic post-break decline of the X-ray afterglow of a single CB in an ISM environment satisfies the closure relation $\alpha_X = \beta_X + 1/2 = \Gamma_X - 1/2$ (or $\alpha_X = \beta_X = \Gamma_X - 1$ for a shot-gun configuration of CBs) independent of the pre-break behaviour, which strongly depends on viewing angle (e.g., Dado and Dar 2012a).

Acknowledgement: We thank an anonymous referee for useful comments and suggestions.

References

- Amati, L., et al. 2007, A&A, 463, 913A
Amati, L., et al. 2008, MNRAS, 391, 577
Barthelmy, S. 1997, http://gcn.gsfc.nasa.gov/gcn_main.html
Beuermann, et al. 1999, A&A, 352, L26
Costa, E., et al. 1997, Nature, 387, 783
Covino, S., et al. 2006, IL Nuovo Cimento B, 121, 1171
Curran, P. A., van der Horst, A. J., & Wijers, R. A. M. J. 2008, MNRAS, 386, 859
Dado, S. & Dar, A., 2012a, ApJ, 761, 148
Dado, S. & Dar, A., 2012b, arXiv:1203.5886 (ApJ, in press)
Dado, S., Dar, A. & De Rújula, A. 2002, A&A, 388, 1079
Dado, S., Dar, A. & De Rújula, A. 2004, A&A, 422, 2004
Dado, S., Dar, A. & De Rújula, A. 2007, ApJ, 663, 400
Dado, S., Dar, A. & De Rújula, A. 2009a, ApJ, 696, 994
Dado, S., Dar, A. & De Rújula, A. 2009b, ApJ, 693, 311
D'Agostini, G. 2005, arXiv:physics/0511182
Dar, A. 1998, ApJ, 500, L93
Dar, A. & De Rújula, A. 2000, arXiv:astro-ph/0008474
Dar, A. & De Rújula, A. 2004, Phys. Rep. 405, 203
D'Avanzo, P., et al. 2012, arXiv:1206.2357

Evans, P. A., et al. 2009, MNRAS, 397, 1177
Frail, D. A., et al. 1997, Nature, 389, 261
Frail, D. A., et al. 2001, ApJ, 562, L55
Fruchter, A. S., et al. 1999, ApJ, 519, L13
Goodman, J., 1986, ApJ, 308, L47
Goodman, J., Dar, A. & Nussinov, S. 1987, ApJ, 314, L7
Gruber, D., et al. 2011, A&A, 531A, 20
Harrison, F. A., et al. 1999, ApJ, 523, L121
Katz, J. 1994, ApJ, 432, L107
Kocevski, D., & Butler, N. 2008, ApJ, 680, 531
Kouveliotou, C., et al. 2004, ApJ, 608, 872.
Kulkarni, S. R., et al. 1999, Nature, 398, 389
Liang, E. W., et al. 2008, ApJ, 675, L528
Margutti, R., et al. 2013, MNRAS, 428, 729
Meegan et al. 1992, Nature, 355, 143
Meszaros, P. & Rees, M. J. 1997, ApJ, 476, 232
Metzger, M. R. et al. 1997, Nature, 387, 878
Mao and Paczynski, B. 1992, ApJ, 388, L45
Nava, L., et al. 2012, MNRAS, 421, 1256
Nousek, J. A., et al. 2006, ApJ, 642, 389
Paczynski, B. 1986, ApJ, 308, L43
Paczynski, B. & Rhoads, J. E. 1993, ApJ, 418, L5
Panaitescu, A., et al. 2006, MNRAS, 369, 2059
Piran, T. 1999, Phys. Rep. 314, 575
Piran, T. 2000, Phys. Rep. 333, 529
Racusin, J. L., et al. 2009, ApJ, 698, 43
Sahu, K. C., et al. 1997, Nature, 387, 476
Sari, R., Piran, T. & Halpern, J. P. 1999, ApJ, 519, L17
Shaviv, N. J. & Dar, A. 1995, ApJ, 447, 863
Stratta, G., et al. 2009, A&A, 494, L9
Van Eerten, H. J., MacFadyen, A. I., & Zhang, W. 2011a, AIP, 1358, 173
van Eerten, F. and MacFadyen, A. 2012, arXiv:1209.1985
van Paradijs, J., et al. 1997, Nature, 386, 686
Wijers, R. A. M. J., Rees, J. & Meszaros, P. 1997, MNRAS, 288, L51
Yonetoku, D., et al. 2010, PASJ, 62, 1495